

## EFT interpretation of low- $p_T$ results

---

**Vasiliki A. Mitsou<sup>a,\*</sup> on behalf of the ATLAS and CMS Collaborations**

*<sup>a</sup>Instituto de Física Corpuscular (IFIC), CSIC – Universitat de València,  
C/ Catedrático José Beltrán 2, E-46980 Paterna (Valencia), Spain*

*E-mail: [vasiliki.mitsou@ific.uv.es](mailto:vasiliki.mitsou@ific.uv.es)*

The observed flavour anomalies in  $b \rightarrow s\ell^+\ell^-$  quark-level transitions offer a platform for indirect searches for signals of New Physics. This contribution focuses on the ATLAS and CMS results from  $B \rightarrow K^*\mu\mu$  angular analyses and the effective field theory interpretation of the low- $p_T$  discrepancies. In addition, it discusses the possibility to also accommodate the muon  $g - 2$  anomaly, in particular the corner of the supersymmetric parameter space left in smuon searches at the LHC.

*11th International Workshop on the CKM Unitarity Triangle (CKM2021)  
22-26 November 2021  
The University of Melbourne, Australia*

---

\*Speaker

## 1. Introduction

Analyses of flavour-changing neutral-current decays are particularly sensitive to the effects of New Physics (NP), since they are highly suppressed in the Standard Model (SM). While there is no direct evidence for NP at the Large Hadron Collider (LHC) [1] up to now, recent measurements of the rare  $b \rightarrow s\ell^+\ell^-$  decays by the LHCb [2] and Belle experiments exhibit consistently discrepancies from the SM predictions of the branching ratios, the angular distributions, and the lepton-flavour-universality (LFU) ratios [3]. In this paper, we report the results of angular analyses performed by the ATLAS [4] and CMS [5] experiments and effective field theory (EFT) interpretations of these and other  $B$ -physics results.

## 2. $B_d^0 \rightarrow K^*\mu^+\mu^-$ angular analyses

ATLAS [6] and CMS [7] performed angular analyses of the decay  $B_d^0 \rightarrow K^*\mu^+\mu^-$  using  $\sim 20 \text{ fb}^{-1}$  of  $pp$  collision data at  $\sqrt{s} = 8 \text{ TeV}$ . The  $K^*$  meson is reconstructed through its decay to  $K^+\pi^-$ , and the  $B$  meson is reconstructed by fitting to a common vertex the tracks from two oppositely charged muon candidates and the tracks from the  $K^*$  decay. The kinematics of the four particles in the final state of the  $B$  meson is described by the invariant mass of the dimuon system,  $q^2$ , and three helicity angles. The full angular differential decay rate is expressed by a set of optimised parameters  $P_i^{(\prime)}$  proposed [8, 9] to reduce the theoretical uncertainties that come from hadronic form factors. Among these parameters, the  $P_5'$  is of particular interest due to the discrepancy of  $> 3\sigma$  with respect to the SM predictions reported by the LHCb [10, 11] and the Belle Collaborations [12].

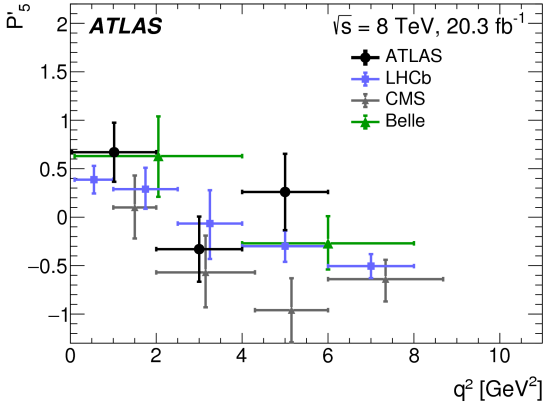


**Figure 1:** The measured values of the  $P_5'$  parameter from ATLAS for  $B_d^0 \rightarrow K^*\mu^+\mu^-$  decays compared with results from LHCb [11], CMS [7], and Belle [13]. From [6].

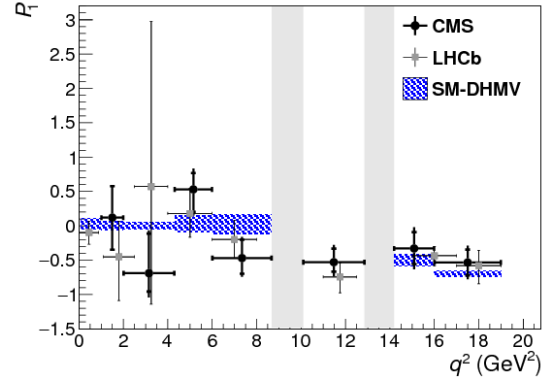


**Figure 2:** CMS measurements of the  $P_1$  angular parameter for  $B_d^0 \rightarrow K^*\mu^+\mu^-$  decays, in comparison to results from the LHCb [11] and Belle [12]. The statistical (total) uncertainties are denoted by the inner (outer) vertical bars. From [7].

The measured values of the  $P_5'$  and  $P_1$  parameters versus  $q^2$  as measured by ATLAS and CMS are shown in Figure 1 and 2, respectively. In Figure 2, the vertical shaded regions correspond to the  $J/\psi$  and  $\psi(2S)$  resonances, while the hatched region shows the SM-DHNV prediction [8, 9] from SM calculations, averaged over each  $q^2$  bin. Moreover, results for other coefficients —  $P_4'$ ,  $P_6'$ ,  $P_8'$  — have been extracted by ATLAS. All results are in agreement with SM expectations within  $3\sigma$ .

The CMS Collaboration has also carried out muon forward-backward asymmetry measurements in the decays  $B^+ \rightarrow K^+ \mu^+ \mu^-$  [14] and  $B^+ \rightarrow K^*(892)^+ \mu^+ \mu^-$  [15]. The results are consistent with previous measurements and they are compatible with the SM predictions.

### 3. Future prospects for $b \rightarrow s \ell \ell$

ATLAS and CMS plan to extend their  $B$ -physics measurements to LFU variables. The latter requires a trigger on electrons and single muons. To this effect, CMS envisages to use  $B$ -parking [16], a technique to dynamically adjust trigger  $p_T$  thresholds during fill to keep high rate despite falling luminosity within fill.

With the High Luminosity LHC phase (HL-LHC), the precision in measuring the  $P'_5$  parameter in  $B_d^0 \rightarrow K^* \mu^+ \mu^-$  decays is expected to improve by a factor of  $\mathcal{O}(10)$ . This is shown in Figure 3 for  $300 \text{ fb}^{-1}$  recorded by CMS [17] and in Figure 4 for an ATLAS dataset of  $3000 \text{ fb}^{-1}$  [18], both at  $\sqrt{s} = 14 \text{ TeV}$ . The ATLAS study [18] includes various muon trigger options; the intermediate  $\mu 10 \mu 6$  trigger scenario is assumed in Figure 4. Alongside, theory predictions are also displayed: CFFMPSV [19], DHMV [20], JC [21]. Precision improvement in other observables, such as  $F_L$ ,  $P_i^{(\prime)}$ , will be possible, too. A finer binning in  $q^2$  will be feasible with  $3000 \text{ fb}^{-1}$ .

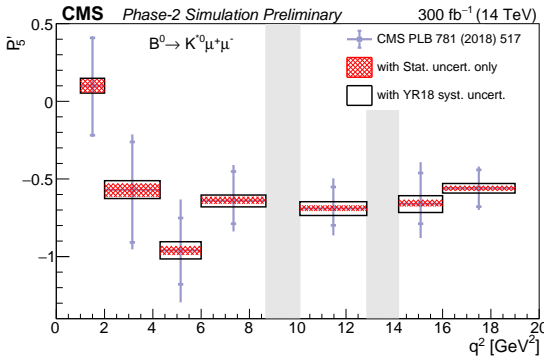


**Figure 3:** Projected statistical (hatched regions) and total (open boxes) CMS uncertainties on the  $P'_5$  parameter vs.  $q^2$  in the Phase-2 scenario with an integrated luminosity of  $300 \text{ fb}^{-1}$ . The CMS Run 1 measurement is shown with inner (outer) vertical bars denoting the statistical (total) uncertainties. From [17].

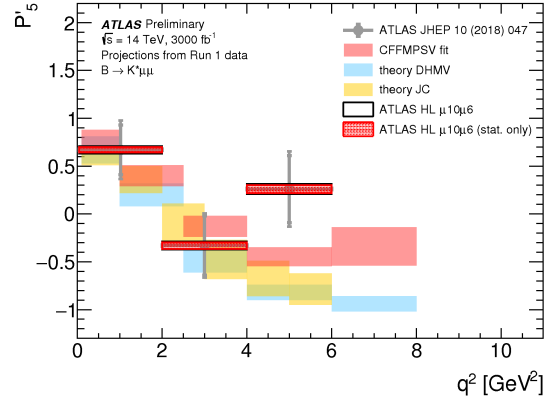


**Figure 4:** Projected ATLAS HL-LHC measurement precision in the  $P'_5$  parameter for the intermediate  $\mu 10 \mu 6$  trigger scenario compared to the ATLAS Run 1 measurement. Both the projected statistical and the total uncertainties are shown. From [18].

### 4. EFT fit to $b \rightarrow s \ell \ell$ data

The new physics effects that may be hidden in low- $p_T$   $B$ -physics measurements can be parameterised by fitting to EFT parameters, the Wilson coefficients  $C_i$ . The following coefficients related to muons are of interest for both SM and NP:

- $C_{9\mu}$ : vector current, dominant contributions to angular and LFU observables, and
- $C_{10\mu}$ : axial current, dominant contributions to  $B_s^0 \rightarrow \mu^+ \mu^-$  and LFU observables,

since global fits indicate a consistent deviation w.r.t. SM, namely a reduction of  $C_9$  for muons, as seen in Figure 5 [22].

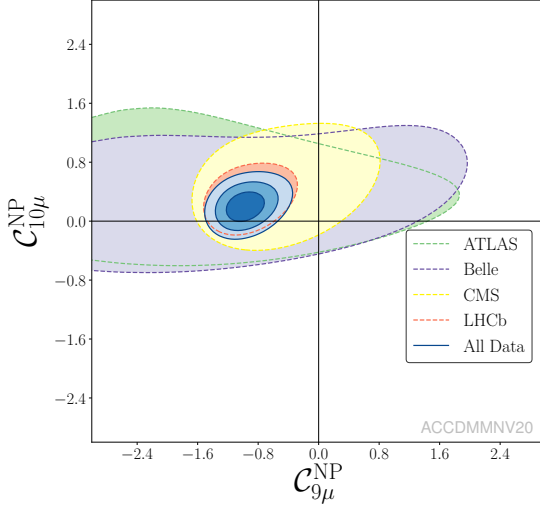


**Figure 5:** Allowed regions in the  $(C_{9\mu}^{NP}, C_{10\mu}^{NP})$  plane for the corresponding 2D hypotheses, using all available rare  $B$  decays observables. From [22].

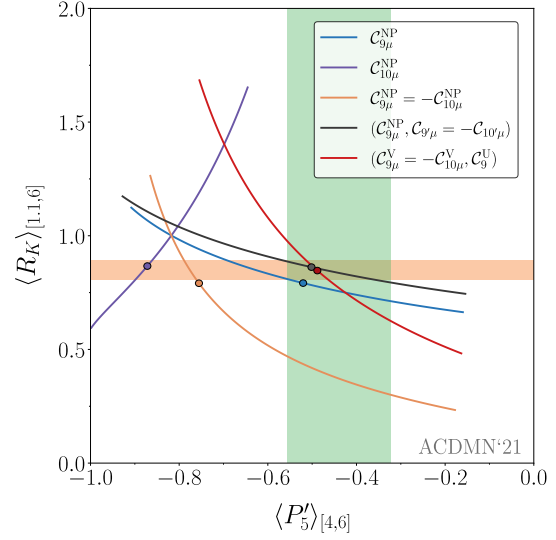


**Figure 6:**  $\langle R_K \rangle_{[1,1,6]}$  versus  $\langle P'_5 \rangle_{[4,6]}$  in five different 1D and 2D EFT scenarios. The numbers in brackets denote  $q^2$  bins. From [23].

Measurements of  $P'_5$  discussed in Section 2 can be combined with LFU variables, such as the  $R_K$ , defined as:

$$R_K = \frac{\mathcal{B}(B^+ \rightarrow K^+ \mu^+ \mu^-)}{\mathcal{B}(B^+ \rightarrow K^+ e^+ e^-)}, \quad (1)$$

to indicate the most favoured EFT scenarios. This ratio was measured by LHCb showing a deficit of the  $\mu$  channel with a  $3\sigma$  significance [24]. Various 1D and 2D scenarios are shown in Figure 6 with the curves corresponding only to the predictions for central values and the dots representing the best-fit points for the fit to all flavour variables. In the case of the 2D scenarios —  $(C_{9\mu}^V = -C_{10\mu}^V, C_9^U)$  and  $(C_{9\mu}^{NP}, C_{9'\mu}^{NP} = -C_{10\mu}^{NP})$  —, the Wilson coefficient not shown is set to its best-fit point. The horizontal and vertical band indicate the LHCb experimental values. The most favoured 1D scenario is the vector coupling to  $\mu$  encoded is  $C_{9\mu}^{NP}$ , which is preferred over the SM with a pull of  $7\sigma$  when fitting all  $b \rightarrow s\mu\mu$  observables [23]. In the 2D scenario  $(C_{9\mu}^V = -C_{10\mu}^V, C_9^U)$ , the coefficient  $C_9^U$  encodes the presence of a LFU NP component to  $C_9$ , i.e.,  $b \rightarrow see$ ,  $b \rightarrow s\mu\mu$  and  $b \rightarrow s\tau\tau$ . The  $C_{9\mu}^V$  and  $C_{10\mu}^V$  are the LFU-violating NP contributions to muon  $C_9$  and  $C_{10}$ . A pattern with right-handed couplings to muons is the  $(C_{9\mu}^{NP}, C_{9'\mu}^{NP} = -C_{10\mu}^{NP})$ , which gives large negative NP contribution to  $C_{9\mu}$ . Many more fits have been performed by other groups [25–32].

On the other hand, the absolute branching ratio of the purely leptonic decay  $B_s^0 \rightarrow \mu^+ \mu^-$  is considered theoretically clean. The related measurements for  $B_{(s)} \rightarrow \mu^+ \mu^-$  made by ATLAS [33], CMS [34] and LHCb [10], as well as their combination [35] is shown in Figure 7. The branching ratio of  $B_s^0 \rightarrow \mu^+ \mu^-$  plays an important role in constraining the Wilson coefficient  $C_{10\mu}$ . As shown in Figure 8, if all rare  $B$  decays are considered, the best fit for the two muon  $C_9$  scenarios is  $(C_9^U, C_{9\mu}^V) = (-0.32, -0.34)$  with a pull of  $5.4\sigma$  [36]. Overall, good agreement is observed between fits of different groups despite different approaches, proving the robustness of the  $b \rightarrow s\ell\ell$  global analyses.

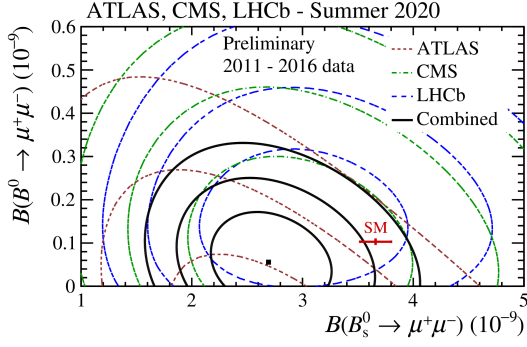


**Figure 7:** 2D likelihood contours of the results for the  $B_s^0 \rightarrow \mu^+\mu^-$  and  $B_d^0 \rightarrow \mu^+\mu^-$  decays for ATLAS [33], CMS [34] and LHCb [10] experiments and their combination for data collected in 2011–2016. For each experiment and for the combination, likelihood contours correspond to the values of  $-2\Delta\ln\mathcal{L} = 2.3, 6.2$ , and  $11.8$ , respectively. The red point shows the SM predictions with their uncertainties. From [35].

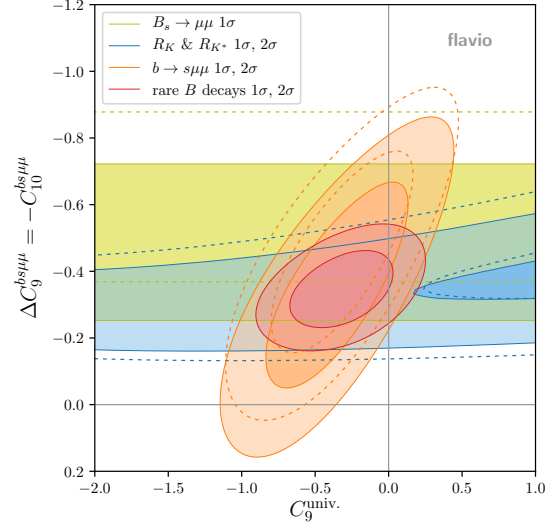


**Figure 8:** Constraints on the Wilson coefficient  $C_9^{univ.}$  vs.  $\Delta C_9^{bs\mu\mu} = -C_{10}^{bs\mu\mu}$ . The dashed lines show the constraints before recent updates. From [36].

## 5. Connection with supersymmetry and muon $g - 2$

Addition of supersymmetric (SUSY) fields brings new penguin and box diagrams in the  $b \rightarrow s\ell\ell$  picture, potentially involving a dark-matter candidate, the lightest neutralino  $\tilde{\chi}_1^0$ . Other possibilities include a (fermionic) chargino and gluino, as well as scalars, such as a stop,  $\tilde{t}$ , a smuon,  $\tilde{\mu}$  or a sneutrino,  $\tilde{\nu}$  [37]. Collider searches have set bounds in various of the involved sparticles [38]. The question remains whether these SUSY scenarios have been ruled out by LHC or not.

Moreover, the still unexplained tension observed in the muon anomalous magnetic moment,  $(g - 2)_\mu$ , initially by the Brookhaven National Laboratory (BNL) E821 experiment [39] has been confirmed recently by the Fermilab Muon  $g - 2$  Collaboration [40]. If the theoretical prediction is considered robust, then the experimental average is  $4.2\sigma$  larger than the SM expectation. SUSY can be a possible explanation via loops involving a  $\tilde{\mu}$  or a  $\tilde{\nu}_\mu$ . Relevant SUSY analyses in this respect include searches for two leptons and missing transverse energy [41] and for soft leptons in compressed-spectra scenarios [42]. ATLAS has compiled recently [43] in Figure 9 the regions excluded by the aforementioned searches on the  $\tilde{\mu}$  production, also highlighting the regions compatible with the  $(g - 2)_\mu$  anomaly. The muon  $g - 2$  values are calculated in the phenomenological Minimal Supersymmetric Standard Model (pMSSM) for various SUSY parameters sensitive to  $(g - 2)_\mu$  and for  $m(\tilde{\chi}_1^0) > 10$  GeV.

Part of the  $(\tilde{\mu}, \tilde{\chi}_1^0)$  parameter space favourable for the  $(g - 2)_\mu$  observed value remains still unconstrained. The flavour anomalies may also be accommodated in these models.

## 6. Summary and prospects

Rare  $b \rightarrow s\ell\ell$  decays are sensitive probes of physics beyond the Standard Model that enter in loop diagrams. Global fits show a consistent set of anomalies across observables and exper-

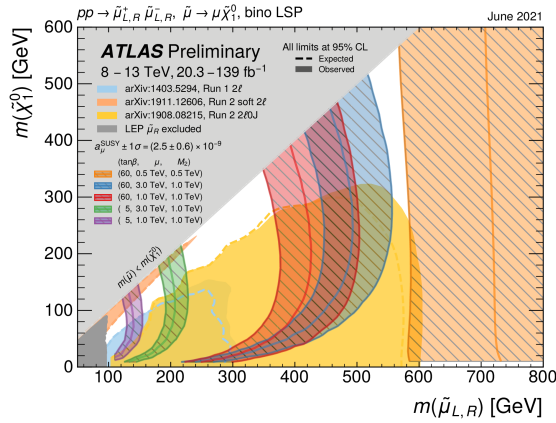


**Figure 9:** Exclusion limits at 95% CL based on 13 TeV data in the  $(\tilde{\mu}, \tilde{\chi}_1^0)$  mass plane for different analyses probing the direct production of  $\tilde{\mu}$  with decays to a  $\mu$  and a bino-like  $\tilde{\chi}_1^0$ . The hatched bands indicate regions compatible with the observed  $(g - 2)_\mu$  anomaly measured by the Fermilab and BNL experiments at the  $\pm 1\sigma$  level, corresponding to the pMSSM parameters specified in the legend. From [43].

iments. ATLAS and CMS are performing, among others, angular-distribution analyses of these decays. Interesting new-physics scenarios explaining these anomalies exist in supersymmetry, also in connection with the  $(g - 2)_\mu$  tension.

CMS and ATLAS are adding capabilities to measure LFU-violating observables:  $R(K^*), R(K)$  in the electron channel and  $R(D), R(D^*)$  in the single-muon channel and the  $\tau$  channel. HL-LHC will bring a  $\sim 10$  times better precision in  $F_L$  and  $P_i^{(\prime)}$  parameters. ATLAS and CMS are exploring more and more  $B$ -physics observables at the LHC.

## Acknowledgments

This work was supported in part by the Generalitat Valenciana via the Project PROMETEO-II/2017/033, by the Spanish MICIU / AEI and the European Union / FEDER via the grant PGC2018-094856-B-I00 and by the CSIC AEPP2021 grant 2021AEP063.

## References

- [1] L. Evans and P. Bryant, *JINST* **3** (2008) S08001.
- [2] LHCb collaboration, *JINST* **3** (2008) S08005.
- [3] LHCb collaboration, *Tests of lepton universality using  $B^0 \rightarrow K_S^0 \ell^+ \ell^-$  and  $B^+ \rightarrow K^{*+} \ell^+ \ell^-$  decays*, [2110.09501](#).
- [4] ATLAS collaboration, *JINST* **3** (2008) S08003.
- [5] CMS collaboration, *JINST* **3** (2008) S08004.
- [6] ATLAS collaboration, *JHEP* **10** (2018) 047 [[1805.04000](#)].
- [7] CMS collaboration, *Phys. Lett. B* **781** (2018) 517 [[1710.02846](#)].
- [8] S. Descotes-Genon, T. Hurth, J. Matias and J. Virto, *JHEP* **05** (2013) 137 [[1303.5794](#)].
- [9] S. Descotes-Genon, J. Matias, M. Ramon and J. Virto, *JHEP* **01** (2013) 048 [[1207.2753](#)].
- [10] LHCb collaboration, *Phys. Rev. Lett.* **118** (2017) 191801 [[1703.05747](#)].
- [11] LHCb collaboration, *JHEP* **02** (2016) 104 [[1512.04442](#)].
- [12] BELLE collaboration, *Phys. Rev. Lett.* **118** (2017) 111801 [[1612.05014](#)].
- [13] BELLE collaboration, in *LHC Ski 2016: A First Discussion of 13 TeV Results*, 4, 2016, [1604.04042](#).
- [14] CMS collaboration, *Phys. Rev. D* **98** (2018) 112011 [[1806.00636](#)].

- [15] CMS collaboration, *JHEP* **04** (2021) 124 [2010.13968].
- [16] CMS collaboration, *Recording and reconstructing 10 billion unbiased  $b$  hadron decays in CMS*, CMS-DP-2019-043, <https://cds.cern.ch/record/2704495>, 2019.
- [17] CMS collaboration, *Study of the expected sensitivity to the  $P'_5$  parameter in the  $B^0 \rightarrow K^{*0} \mu^+ \mu^-$  decay at the HL-LHC*, CMS-PAS-FTR-18-033, <https://cds.cern.ch/record/2651298>, 2018.
- [18] ATLAS collaboration,  *$B_d^0 \rightarrow K^{*0} \mu \mu$  angular analysis prospects with the upgraded ATLAS detector at the HL-LHC*, ATL-PHYS-PUB-2019-003, <https://cds.cern.ch/record/2654519>, 2019.
- [19] M. Ciuchini, M. Fedele, E. Franco, S. Mishima, A. Paul, L. Silvestrini et al., *JHEP* **06** (2016) 116 [1512.07157].
- [20] S. Descotes-Genon, L. Hofer, J. Matias and J. Virto, *JHEP* **12** (2014) 125 [1407.8526].
- [21] S. Jäger and J. Martin Camalich, *JHEP* **05** (2013) 043 [1212.2263].
- [22] M. Algueró, B. Capdevila, A. Crivellin, S. Descotes-Genon, P. Masjuan, J. Matias et al., *Eur. Phys. J. C* **79** (2019) 714 [1903.09578]. [Addendum: *Eur.Phys.J.C* 80, 511 (2020)].
- [23] M. Algueró, B. Capdevila, S. Descotes-Genon, J. Matias and M. Novoa-Brunet, 4, 2021, 2104.08921.
- [24] LHCb collaboration, *Test of lepton universality in beauty-quark decays*, 2103.11769.
- [25] M. Ciuchini, M. Fedele, E. Franco, A. Paul, L. Silvestrini and M. Valli, *Phys. Rev. D* **103** (2021) 015030 [2011.01212].
- [26] T. Hurth, F. Mahmoudi, D. M. Santos and S. Neshatpour, *Phys. Lett. B* **824** (2022) 136838 [2104.10058].
- [27] L.-S. Geng, B. Grinstein, S. Jäger, S.-Y. Li, J. Martin Camalich and R.-X. Shi, *Phys. Rev. D* **104** (2021) 035029 [2103.12738].
- [28] A. K. Alok, A. Dighe, S. Gangal and D. Kumar, *JHEP* **06** (2019) 089 [1903.09617].
- [29] A. Datta, J. Kumar and D. London, *Phys. Lett. B* **797** (2019) 134858 [1903.10086].
- [30] K. Kowalska, D. Kumar and E. M. Sessolo, *Eur. Phys. J. C* **79** (2019) 840 [1903.10932].
- [31] G. D'Amico, M. Nardecchia, P. Panci, F. Sannino, A. Strumia, R. Torre et al., *JHEP* **09** (2017) 010 [1704.05438].
- [32] G. Hiller and I. Nisandzic, *Phys. Rev. D* **96** (2017) 035003 [1704.05444].
- [33] ATLAS collaboration, *JHEP* **04** (2019) 098 [1812.03017].
- [34] CMS collaboration, *JHEP* **04** (2020) 188 [1910.12127].
- [35] ATLAS collaboration, *Combination of the ATLAS, CMS and LHCb results on the  $B_{(s)}^0 \rightarrow \mu^+ \mu^-$  decays*, ATLAS-CONF-2020-049, <https://cds.cern.ch/record/2728059>, 8, 2020.
- [36] W. Altmannshofer and P. Stangl, *Eur. Phys. J. C* **81** (2021) 952 [2103.13370].
- [37] M. A. Boussejra and F. Mahmoudi, in *European Physical Society Conference on High Energy Physics 2021*, 11, 2021, 2111.07938.
- [38] V. A. Mitsou, *PoS CORFU2019* (2020) 050.
- [39] MUON G-2 collaboration, *Phys. Rev. D* **73** (2006) 072003 [hep-ex/0602035].
- [40] MUON G-2 collaboration, *Phys. Rev. Lett.* **126** (2021) 141801 [2104.03281].
- [41] ATLAS collaboration, *Eur. Phys. J. C* **80** (2020) 123 [1908.08215].
- [42] ATLAS collaboration, *Phys. Rev. D* **101** (2020) 052005 [1911.12606].
- [43] ATLAS collaboration, *SUSY Summary Plots June 2021*, ATL-PHYS-PUB-2021-019, <https://cds.cern.ch/record/2771785>, 2021.